Dual Predation by Bacteriophage and *Bdellovibrio* Can Eradicate *E. coli* Prey in Situations Where Single Predation Cannot

Laura Hobley,[a*] J. Kimberley Summers,[b] Rob Till,[a] David S. Milner,[a*] Robert J. Atterbury,[a*] Amy Stroud,[a] Michael J. Capeness,[a*] Stephanie Gray,[a] Andreas Leidenroth,[a] Carey Lambert,[a] Ian Connerton,[c] Jamie Twycross,[d] Michelle Baker,[a*] Jess Tyson,[a] Jan-Ulrich Kreft,[b#] R. Elizabeth Sockett[a#]

[a]School of Life Sciences, University of Nottingham, Nottingham, UK

[b]Institute of Microbiology and Infection & Centre for Computational Biology & School of Biosciences, University of Birmingham, Birmingham, UK

[c]School of Biosciences, University of Nottingham, Loughborough, UK

[d]School of Computer Science, University of Nottingham, Nottingham, UK

Running head: Phage-*Bdellovibrio* co-predation

Address correspondence to R. Elizabeth Sockett liz.sockett@nottingham.ac.uk and Jan-Ulrich Kreft J.Kreft@bham.ac.uk

L.H. and J.K.S. contributed equally to this work

LH was the lead experimentalist for the wet bench work, JKS was the lead mathematical modeller, these were equally important contributions to the paper and so authors are listed alphabetically by surname as joint first author.

* Present Address: Laura Hobley, School of Biosciences, University of Nottingham, Loughborough, UK; Michelle Baker, School of Biosciences, University of Nottingham, Loughborough, UK; David S. Milner, School of Biosciences, University of Exeter, Exeter, UK; Robert J. Atterbury, School of Veterinary Medicine and Science, University of Nottingham,

Loughborough, UK; Michael J. Capeness, School of Biological Sciences, University of Edinburgh, Edinburgh, UK.

Word Count: Abstract: 250. Importance: 117. Main text: 6938

ABSTRACT

Bacteria are preyed upon by diverse microbial predators including bacteriophage and predatory bacteria, such as *Bdellovibrio bacteriovorus*. Whilst bacteriophage are used as antimicrobial therapies in Eastern Europe, and are being applied for compassionate use in the United States, predatory bacteria are only just beginning to reveal their potential therapeutic uses. However, predation by either predator type can falter due to different adaptations arising in the prey bacteria. When testing poultry farm wastewater for novel *Bdellovibrio* isolates on *E. coli* prey lawns, individual composite plaques were isolated, containing both an RTP-like-phage and a *B. bacteriovorus* strain and showing central prey lysis and halos of extra lysis. Combining the purified phage with a lab strain of *B. bacteriovorus* HD100 recapitulated halo-ed plaques, and increased killing of the *E. coli* prey in liquid culture, showing effective side-by-side action of these predators, compared to their actions alone. Using Approximate Bayesian Computation to select the best fitting from a variety of different mathematical models demonstrated that the experimental data could only be explained by assuming the existence of three prey phenotypes: (1) sensitive to both predators, (2) genetically resistant to phage only and (3) plastic resistant to *B. bacteriovorus* only. Although each predator reduces prey availability for the other, high phage numbers did not abolish *B. bacteriovorus* predation so both predators are competent to co-exist and are causing different selective pressures on the bacterial surface while, in tandem, controlling prey bacterial numbers efficiently. This suggests that combinatorial predator therapy could overcome problems of phage resistance.

52 **IMPORTANCE**

53 With increasing levels of antibiotic resistance, the development of alternative anti-bacterial
54 therapies is urgently needed. Two potential alternatives are bacteriophage and predatory
55 bacteria. Bacteriophage therapy has been used but prey/host specificity and the rapid
56 acquisition of bacterial resistance to bacteriophage are practical considerations. Predatory
57 bacteria are of interest due to their broad Gram-negative bacterial prey-range, and the lack
58 of simple resistance mechanisms. Here, a bacteriophage and a strain of *Bdellovibrio*
59 *bacteriovorus*, preyed side-by-side on a population of *E. coli* causing significantly greater
60 decrease in prey numbers than either alone. Such combinatorial predator therapy may have
61 greater potential than individual predators as prey surface changes selected for by each
62 predator do not protect prey against the other predator.

63

64 KEYWORDS *Bdellovibrio*, bacteriophage, RTP phage, predation, co-operation, predator prey
65 models, mathematical modelling, Approximate Bayesian Computation

66

67 **INTRODUCTION**

68 Rapidly rising levels of antimicrobial resistance in Gram-negative bacterial pathogens
69 has highlighted the urgent need for the development of alternative forms of antibacterial
70 therapies (1) and the World Health Organisation has listed several as critically urgent for
71 new therapeutics. Many Gram-negative pathogens can be killed by a variety of
72 bacteriophage ('phage') and by predatory bacteria including *Bdellovibrio bacteriovorus* (2,
73 3). Bacteriophage have been used regularly in Eastern Europe and Russia as antimicrobial
74 therapies (4). However, the development of bacterial resistance to bacteriophage can occur
75 rapidly both *in vitro* and *in vivo* by receptor gene mutations (5-7), leading to the
76 requirement for, and development of, phage cocktails for therapeutic purposes, including
77 recent compassionate treatment use (8, 9). *Bdellovibrio* have recently been the subject of a
78 number of *in vivo* studies to test their efficacy in animals (10-12), but have yet to be trialled
79 for use in humans. Unlike bacteriophage, there are no known simple receptor gene
80 mechanisms for resistance.

81 Bacteriophage are obligate intracellular predators that can be found in environments
82 wherever susceptible bacteria are available; over 95% of phage isolates described to date
83 belong to the order Caudovirales or "tailed phage" (13). The tails of these phage attach to
84 receptors on the surface of the host bacterium including flagella (14), lipopolysaccharide
85 (15) or outer membrane proteins (16). Due to the specific nature of the receptor for phage
86 attachment, the host range of each phage is typically quite small, determined by the
87 prevalence and conservation of phage receptors in bacterial populations (17). The cellular
88 machinery of the bacterium is rapidly hijacked by the phage, after injection of the viral
89 genome, and redirected to synthesize and assemble new phage virions that are released to
90 start a new infection cycle (2). Host resistance against bacteriophage infection falls within

four general categories: inhibition of adsorption; blocking injection of the viral genome; recognition and restriction modification of bacterial DNA and inhibition of the transcription and replication of phage DNA (18, 19)

B. bacteriovorus predation is a biphasic process, consisting of a flagellate, rapidly swimming phase, before colliding with, attaching to and invading Gram-negative bacteria (which can be either actively growing or in stationary phase) (20). *B. bacteriovorus* invade prey cells by interacting with the outer membrane, creating a pore in the outer membrane and wall, through which they enter into the prey cell periplasm, sealing the pore behind them, forming a rounded structure called a bdelloplast (20). Unlike bacteriophage, which hijack prey replication machinery for their own replication, *Bdellovibrio* invasion results in the rapid death of the prey cell (20, 21). Periplasmic *Bdellovibrio* secrete many enzymes into the prey cell cytoplasm, using the cytoplasmic contents for growth. The *Bdellovibrio* elongates, divides into multiple progeny cells, lyses the prey bdelloplast and is released (22).

By growing intracellularly, the *Bdellovibrio* is within an enclosed niche and does not have to compete with other bacteria for resources. The only known protection against predation is the synthesis of a paracrystalline S-layer by prey cells, however, *Bdellovibrio* are still able to prey on S-layer+ cells should there be any patchiness to the S-layer (23). It has been observed that, in laboratory culture, not all prey bacteria are killed by *Bdellovibrio*, a small population exhibits a “plastic” resistance phenotype; when removed from predators and allowed to grow, the resulting cells are as sensitive to *Bdellovibrio* predation as the original prey population (24). Prey resistance to antibiotics does not result in resistance to *Bdellovibrio* predation as has been shown in multiple studies looking at drug-resistant Gram-negative pathogens (25, 26). Although well-known for their predatory nature, *B. bacteriovorus* are not obligate predators, approximately one in a million *Bdellovibrio* from a

115 predatory culture can be grown axenically, prey/host-independently (HI), on complex media
116 without prey (27).

117 Mathematical modelling of bacterial predation is being increasingly applied to
118 understanding predation kinetics of either bacteriophage or *Bdellovibrio;* however
119 modelling of predation by both types of predators on the same prey species has not yet
120 been reported. Bacteriophage predation has been the subject of numerous studies,
121 reviewed in (7, 28), with the models becoming increasingly complex through the inclusion of
122 the effects of the rise of prey resistance (6), altered nutrient availability, multiple bacterial
123 species and more (28). Modelling of *Bdellovibrio* predation is more limited, having started
124 from the original Lotka-Volterra equations (29), via considering a delay between prey death
125 and predator birth (30) to models that consider the bdelloplast stage as a separate
126 population rather than just as a delay (31-34). Few papers considered decoys (33, 34) and
127 one of these integrated experiments and adjusted the model to match the experiments
128 (33). Other models considered the effect of a refuge on predation (32), the effect of serum
129 and "plastic" resistance of prey to *Bdellovibrio* on predation (31), or how predation
130 efficiency depends on prey size and other factors (35).

131 Here, during sampling standing water on a poultry farm for novel *Bdellovibrio*
132 isolates, single halo-ed plaques were observed on *E. coli* prey lawns. Within each halo-ed
133 plaque was both a predatory *Bdellovibrio bacteriovorus* and a co-isolated bacteriophage. In
134 this paper we use 'prey' as a unified term that encompasses both prey for *Bdellovibrio* and
135 host for bacteriophage, as in this work a single bacterium, *E. coli*, acts as both prey and host
136 and we are comparing the action of two different predators.

137 The phage genome was partially sequenced and shown to be homologous to that of
138 a rosette-tailed-phage (RTP) (36). The RTP phage family differ in tail structure, but are

139 related to the T1 phages, the receptor for some of which is a component of the *E. coli* outer
140 membrane and host-resistance is reported to arise frequently (36).

141 Our experimental analysis of predation kinetics revealed that when both predators
142 were combined in one culture with *E. coli* prey, complete prey lysis was achieved in 48
143 hours. This was in contrast to cultures containing either of the single predators where prey
144 remained; with phage alone the remaining prey were phage-resistant, whilst with
145 *Bdellovibrio* alone a subpopulation of prey remained but no acquisition of genetic resistance
146 occurred. Mathematical modelling of this experimental system revealed that both phage
147 resistance and the plastic resistance to *Bdellovibrio* predation arose in the *E. coli* prey
148 population, and that the two predators were most likely acting independently and
149 competitively rather than cooperatively. This work shows that two bacterial predators can
150 be co-isolated from the environment, co-exist in lab cultures, and when applied in
151 combination can result in greater killing of the prey bacterial population than by either
152 predator alone; suggesting that *Bdellovibrio*-phage combinations may be a successful
153 approach towards therapeutic antibacterials.

154

155 **RESULTS**

156 **Isolation of environmental *B. bacteriovorus* and associated bacteriophage.**

157 When isolating *Bdellovibrio* from 0.45 μm filtrates of standing water on a poultry farm, one
158 isolate rapidly lysed offered *E. coli* lab cultures, and repeatedly produced plaques with large
159 "halos" around them on prey lawns (Fig. 1A). These plaques contained characteristic small,
160 highly-motile *B. bacteriovorus*-like bacteria (Fig. 1B), and "bdelloplasts" - infected *E. coli*
161 prey cells containing live *B. bacteriovorus*. Sequencing and alignment of the 16S rRNA gene
162 amplified from predatory *Bdellovibrio* purified from a single isolated "halo-ed" plaque

showed that the *Bdellovibrio* was a member of the *B. bacteriovorus* species, and its 16S rRNA sequence (GenBank accession no: GQ427200.1) to be 99% identical to that of the type strain HD100 (37). Therefore the isolated *Bdellovibrio* was named *B. bacteriovorus* angelus, due to the initial halo-ed appearance of the plaques from which it was isolated.

Predatory cultures derived from individual "halo-ed" plaques, when filtered through 0.22 μm filters, which retain *B. bacteriovorus*, were found to contain an agent that lysed *E. coli* giving different cell debris (without the rounded bdelloplasts). The concentrated filtrate showed several prominent protein bands on SDS PAGE (Fig. S1A). One of these bands (of approximately 30 kDa) was found, by MALDI QToF MS, (Fig. S1B) to contain 5 peptides which were homologous to the 34 kDa protein RTP27 (GenBank accession no: CAJ42231.1) of a rosette-tailed phage (RTP) of *E. coli* (36). Simultaneous electron microscopy of the 0.22 μm filtrate revealed many phage particles with curved tails that resembled RTP, without such a pronounced rosette on the tail (Fig. 1C). The phage was given the abbreviated name "halo" and the 46 kDa double stranded DNA phage genome was purified and 7 kb of it was sequenced (GenBank GQ495225.1 bacteriophage halo named RES2009a) and compared in BLAST to other phage genomes. The best matches were to phage genomes belonging to the "rtpvirus" genus, including the characterised RTP phage (EMBL AM156909.1) (36). The phage halo was plaque-purified away from the *B. bacteriovorus*, using a kanamycin resistant *E. coli* as prey (as *B. bacteriovorus* angelus was found to be kanamycin sensitive - as is the type strain HD100) and so was inhibited from predatorily replicating in the Kn^R *E. coli* in the presence of the antibiotic).

Thus *B. bacteriovorus* angelus and bacteriophage halo had been co-isolated, from the same environment, via single "halo-ed" plaques in bacterial prey lawns, in which both

predators were preying, side by side, upon the same offered *E. coli* population and thus it is possible that they prey similarly in the natural environment.

***E. coli* resistance to bacteriophage halo occurred rapidly.**

Rapid phage resistance was observed in *E. coli* S17-1 cultures that were preyed upon by the bacteriophage halo alone; with a persistent level of *E. coli* remaining after 16 hours of infection (see Fig. 2B for an example from later growth experiments). Two independently-derived phage-resistant *E. coli* cultures, (F & G), were isolated by plating out the remaining *E. coli* prey cells from these 16 hour cultures – preyed upon by the phage alone. The two isolates were verified as being phage-resistant by being tested for phage predation again. Genome sequencing of each isolate, alongside the original *E. coli* S17-1 strain used in the experiments, was performed to identify the mutations that resulted in phage resistance. This revealed (Table 1) that two different IS4 transposase insertions had occurred and been selected for in the genomes of resistant strains F and G within the same gene - encoding the ligand-gated outer membrane porin FhuA responsible for ferric hydroxamate uptake through the outer membrane (36). The FhuA protein is known to act as a receptor for other phages and is likely to be the receptor for phage halo (38).

The two halo-phage resistant *E. coli* derivatives grew at similar rates to the parental *E. coli* S17-1 strain. Using the phage resistant *E. coli* as prey in lawns in overlay plates allowed for plaque formation by, and subsequent purification of, the *B. bacteriovorus* angelus isolate away from the phage (Fig. S2A), as phage resistance did not confer any resistance to predation by *B. bacteriovorus*.

We also verified (data not shown) that *B. bacteriovorus* is not susceptible to lytic or lysogenic infection by bacteriophage halo in two tests. Firstly, using host-independent

derivatives of both *B. bacteriovorus* angelus and HD100 (isolate HID13 (21)) as prey in lawns onto which bacteriophage halo was added. No zones of clearing were observed, even after prolonged incubation. Secondly, after addition of bacteriophage to liquid cultures of pure attack-phase *B. bacteriovorus* angelus, or HD100, no evidence of phage infection was seen when observed microscopically or enumerated. Thus *B. bacteriovorus* itself is not susceptible to the bacteriophage halo during either predatory or prey-independent lifecycles.

Experimental predation by combined *B. bacteriovorus* HD100 and halo-phage predators eradicates *E. coli* prey unlike single predators.

To test the effects of predation by the two predators on a single prey population at the same time, the kinetics of predation by equal numbers of phage alone, *B. bacteriovorus* alone and *B. bacteriovorus* plus phage on *E. coli* S17-1 was measured alongside an *E. coli* with buffer control (Fig. 2A-D) using methods as detailed below. We had found no specific association between the phage and the environmental *B. bacteriovorus* co-isolate as mixing the purified halo phage and pure *B. bacteriovorus* angelus or *B. bacteriovorus* HD100 suspensions together both reconstituted halo-ed plaques on a lawn of *E. coli* prey. Having noted that predation rates in liquid cultures of each of the two *B. bacteriovorus* strains angelus and HD100 were the same, but that HD100 forms larger (and hence more visible and countable) plaques, the HD100 strain was used in predation kinetics studies on *E. coli* with or without the phage.

As phage are usually grown in log-phase prey cultures in broth and *B. bacteriovorus* on stationary phase prey in calcium HEPES buffer, a “compromise” late log-phase *E. coli* prey, of starting OD_{600nm} 0.75, was used with a mean initial *E. coli* population of 2.9×10^8

234 cfu/ml. Deliberate inclusion of an equal volume of background YT medium used for the *E.*
235 *coli* pre-culture in the CaHEPES buffer gave a low nutrient environment, which allowed for *E.*
236 *coli* viability throughout the 48 hour test period (Fig. 2B).
237
238 The overall kinetics of the 48 hour experiments were followed by optical density at 600 nm
239 (OD_{600}; Fig. 2A) and viable counts (Fig. 2B,C,D), which indicated that, during the first 24 hour
240 period, *E. coli* was killed more slowly by *B. bacteriovorus*, than when preyed upon by both *B.*
241 *bacteriovorus* and bacteriophage halo together (Fig. 2B). When incubated solely with the
242 bacteriophage halo, the *E. coli* numbers decreased rapidly, reaching the lowest prey density
243 of 2.1×10^3 cfu/ml at 6-8 hours; after which the *E. coli* population began to rise, due to the
244 increase in phage resistant cells within the prey population (Fig. 2B). Interestingly, when the
245 prey were incubated with both the phage and the *B. bacteriovorus*, this increase in prey
246 numbers did not occur, instead the *E. coli* population was eradicated after 14 hours,
247 dropping to below detectable numbers (less than 10 cfu/ml) (Fig. 2B). The phage and *B.*
248 *bacteriovorus* population numbers were lower (by 10-fold and 100-fold respectively at the
249 48 hour timepoints) in the combined culture, likely due to the reduced numbers of prey
250 available to each predator population (Fig. 2C and D). It was noteworthy that adding an
251 equal number of 5×10^6 pfu/ml of the other predator, each with the potential to kill and
252 remove an *E. coli* cell from the available prey pool, caused 10 fold less reduction in phage
253 numbers than in *B. bacteriovorus* numbers. This may be due to more rapid kinetics of *E. coli*
254 predation by phage versus the slower kinetics of killing by *B. bacteriovorus*. As the
255 emergence of genetic or plastic resistance, respectively to the two different predators,
256 would be expected to have a major effect, we modelled these processes mathematically to
257 investigate them further.

258

259 **Mathematical modelling of co-predation.** Modelling started from a one prey and one
260 predator model (35). A bacteriophage was added as a second predator to build the base
261 model of the experimental system (Fig. 3). This base model has one (*E.coli*) prey type (N)
262 and two consumers of the prey, the Predator *B. bacteriovorus* (P) and the Virus
263 bacteriophage halo (V). Both attack and enter the prey to form a distinct stage, thereby
264 removing prey and predator from their respective populations. When *B. bacteriovorus*
265 enters the prey, a bdelloplast (B) is formed. When the phage infects the prey, an Infected
266 prey (I) is formed. Upon lysis of B or I, resources enabling regrowth of prey called M for
267 Medium are released, together with the respective predator offspring.

268 The combined resource M is needed because the experimental data shows regrowth
269 of *E. coli* during halophage predation (Fig. 2B). Altogether, the base model (Fig 3A) has 6
270 variables shown as circles. Processes are shown as arrows and terms of the equations in Fig.
271 3. These are: (i) prey growth by consumption of medium, (ii) predation of prey by available
272 *B. bacteriovorus* to yield the Bdelloplast, (iii) predation by free bacteriophage halo (virus) to
273 yield the Infected prey, (iv) maturation (replication and development) of *B. bacteriovorus*
274 within the bdelloplast, (v) maturation of the bacteriophage (virus) within the Infected prey,
275 (vi) lysis of bdelloplast which yields free replicated *B. bacteriovorus* and releases nutrients
276 which replenish Medium, (vii) lysis of Infected prey which yields free Virus and also releases
277 nutrients which replenish Medium. The nutrients remaining were not sufficient to produce
278 further whole progeny *B. bacteriovorus* or more phage, but will be a small residue of what
279 did constitute the original prey cell as most nutrients were used in producing *B.*
280 *bacteriovorus* or phage progeny. As mentioned above the Medium does allow some limited
281 growth of the prey.

282 We also included (viii) mortality for *B. bacteriovorus* as this was evident from Fig. 2C
283 and is well known from the literature (33, 39). We did not include mortality for *E. coli* and
284 the halophage since the data showed no evidence for this during the 48 h experimental
285 time-period (no statistically significant trend; Fig. 2B and D).
286 From this base model (Fig 3), we generated a family of related models, adding additional
287 variables and processes step by step and testing different mechanisms for the transitions
288 between entities (Fig. 4). We then used Bayesian inference to select, in several stages, the
289 model variant that best fitted the population dynamics observed in the experiments (Fig. 5,
290 see also Fig. S6 demonstrating reproducibility). A full description of the model variants and
291 the Approximate Bayesian Computation process for model selection and parameter
292 inference is given in Supplemental Text.
293 Competing the top level model variants with one, two, three or four prey types (Fig.
294 4C) gave clear results (Fig. 5A). The model variant N1 with prey sensitive to both predators
295 (N_S) and variant N2 with only N_S and bacteriophage resistant prey (N_R) were not supported
296 by the experimental data at all. The variant N3 with N_S, N_R and prey exhibiting the "plastic"
297 phenotypic resistance to *B. bacteriovorus* predation (N_P), was best supported by the
298 experimental data, while variant N4 including the double resistant prey (N_D) was less
299 supported (Fig. 5A). N3 and N4 are nested models with the same number of parameters, so
300 fitting variant N4 is not intrinsically more difficult. Using the parameter values generated by
301 fitting either of the variants N3 or N4, predicted similarly low levels of double resistant prey
302 at the end of the experiment when applied to the equations of variant N4. Variant N4 fitted
303 to all data predicted 0.26 cfu/ml while the same variant using parameters from fitting
304 variant N3 to all data predicted 0.0084 cfu/ml. Both are well below the detection threshold
305 in the experiments (10 cfu/ml). Variant N4 predicts double resistance to occur, albeit at a

very low level, however the data could not provide information to constrain this density. Due to these considerations and the aim to choose the minimal adequate model, the N3 model variant was selected for further study.

After selecting this three prey type N3 model, we tested various sub-models based on different ways in which the sensitive prey type converts to the type with plastic phenotypic resistance to *B. bacteriovorus* and back (Fig. 4Di). The simplest assumption is that forward and backward conversion occur spontaneously at certain rates, without any external triggers (intrinsic conversion both ways, variant I). This was not supported by the data (Fig. 5B). Another model variant replaces the intrinsic back conversion with a growth-coupled conversion (variant IG). This variant was well supported by the data. A third variant replaces the intrinsic conversion by a signal-triggered conversion to plastic resistance (variant S). At this initial stage in the modelling, the signal was assumed to be generated by the lysis of bdelloplasts and phage infected cells. Plastic resistance has been previously described (24) as developing to *B. bacteriovorus* in predatory cultures, due to (as yet unidentified) molecular signals changing prey metabolism/development but it is not due to genetic changes in the prey as when those prey are grown in new cultures and re-challenged with *B. bacteriovorus* they are susceptible once more (21). This variant S had some support from the data (Fig. 5B). Hence, we tested whether a combination of the two supported variants would fit better. This combined variant SG, with signal triggered conversion to plastic resistance plus growth-coupled back conversion, was better supported by the data than its parental variants (Fig. 5C).

Following this, we compared variants where the source of the signal was interaction of prey with phage only, or *B. bacteriovorus* only, or both (Fig. 5D). Since there was no evidence for phage involvement, and the two variants with *B. bacteriovorus* involvement

were about equally supported, we concluded that *B. bacteriovorus* interaction with prey was sufficient to generate the signal for plastic resistance.

Likewise, we looked in the model at different ways in which the phage resistant prey arise (Fig. 4Dii). We compared the simpler sub-models where some phage resistant prey are already present at the beginning of the experiment, as in the classic fluctuation test of Luria and Delbrück (40), or only develop as *de novo* mutations during the experiment with the combined sub-model that had both pre-existing and *de novo* mutations. This combined model variant was best supported by the data and *de novo* developing mutations alone are insufficient to explain the data (Fig. 5E).

Modelling predation-rate saturation

After finding the 'best' or most appropriate model variant for prey type conversions, we looked at the low level model variants (Fig. 4E) where details of the model are varied but not the number of prey types and their conversion. One such detail is whether the predation rate saturates at higher prey density or not (Fig. 4E). Only the variant assuming no saturation of predation rate for the phage but saturation of predation rate for *B. bacteriovorus* was supported by the data (Fig. 5F). This does not mean that phage predation would not saturate at higher prey densities than we investigated in this study, but that the bacterial predator saturates at lower prey densities than the phage (see parameters in Table S1). This is expected as the longer the prey 'handling time' for a predator, the more its response will saturate when prey becomes abundant (41). It is well known that *B. bacteriovorus* takes longer to attach and enter its prey periplasm than phage (20) and our results support this (42). Lack of saturation facilitates the observed rapid initial prey killing by phage (Fig. 2). We did not consider saturation effects at high phage densities in this study because there was little information in the data from experiments that concentrated on

later timepoints and the rise of phage resistance to parameterise phage saturation (there is only a brief interval with high phage density while sensitive prey are available, see Fig. 2B & D). We did however model different initial prey densities as shown in Figure S8, see below.

The final model shows effective side-by-side action of dual predators.

The final, most appropriate model variant was then fitted to all the data (Fig. 6A-D). We explain in Supplemental Text how we used Principal Component Analysis to objectively select a typical parameter set out of the hundreds of accepted fits. The final model fits the prey dynamics well, apart from the exact kinetics of the decline of prey in the presence of *B. bacteriovorus* as the only predator (Fig. 6B) where prey density does not drop as gradually in the model as in the experiments. Despite trying many variants of prey type conversions, we could not find any variant that would give a better fit to this more gradual decline of prey without making the fit to other parts of the data much worse, so Fig. 6A-D shows the best fit we could obtain.

We also compared the fit of this final model to all data (Fig. 6A-D) with the fit of the same model to all data, excluding that from two predators acting on one prey (Fig. 6E-H). The two fits are almost the same. This means that the experimental results can be explained without invoking any direct interactions between the two predators.

Dependence on initial densities.

To understand the dependence of predation success on the initial densities of prey and predators, we used the model to predict the outcome if we varied one population at a time, increasing as well as decreasing initial densities 10-fold (Fig. S8). The time series of the three related traces (10-fold lower, normal, 10-fold higher initial densities) showed similar

qualitative behaviour for cases with prey only and prey with a single predator. Here, the three traces either converged in the end or their separation was less than the 10-fold initial separation. Prey could survive during dual predation if (i) the initial density of prey was too high, or (ii) the initial density of *B. bacteriovorus* was too low or (iii) the initial density of the phage was too high (Fig. S8F-H). The model can thus identify suitable densities of the predators to add for effective predation.

Modelling reveals interactions of sub-populations of predators and prey

The modelling allowed insights into the different sub-populations that comprised the observed total bacterial populations (Fig. 6I-L). In the simulated *B. bacteriovorus*-only predation, the *B. bacteriovorus* population is evenly split between free *B. bacteriovorus* and bdelloplasts from 2 to 20 hours. Afterwards, the bdelloplasts decline exponentially while free *B. bacteriovorus* increase a little (due to progeny release from bdelloplasts) and then decline again due to their mortality (Fig. 6J). Both the fully-susceptible and phage-resistant prey populations plummet at 20 hours, when the plastic resistant prey has reached a plateau (Fig. 6J). In the simulated phage-only predation, sensitive prey rapidly dropped in the first 6 hours, afterwards the phage resistant prey increased exponentially until reaching a plateau (Fig. 6K). In the simulated dual predation, the phage is mostly responsible for the rapid drop of the susceptible prey and the removal of the intermittently arising plastic *B. bacteriovorus* resistant prey, whilst *B. bacteriovorus* is responsible for the removal of the phage resistant prey. All three prey populations are eradicated by the two predators together (Fig. 6K).

DISCUSSION

When attempting to isolate *Bdellovibrio* strains from environmental sources, a sample of chicken farm wastewater gave halo-ed plaques on lawns of *E. coli*, due to the combined predation by the new strain of *B. bacteriovorus*, which we named angelus, and an RTP-like bacteriophage, which we named halo. The combined predation was also produced by the addition of bacteriophage halo to lab strain *B. bacteriovorus* HD100. We combined both experimental and mathematical modelling approaches to unravel the dynamics of this combinatorial predation, showing that a combination of two microbial predators eradicated a single pathogenic bacterial species in conditions when each alone did not. The modelling suggested that *B. bacteriovorus* killed all the phage resistant prey types and the phage halo killed all the plastically *B. bacteriovorus*-resistant prey. This suggests that combinatorial predator therapy may be one approach to tackle the problem of phage resistance in phage therapy treatments.

Although found co-associated in nature, the RTP-family phage halo did not attach to, lyse or lysogenise the *B. bacteriovorus*, but was found to prey alongside it on *E. coli* in experimental lawns, producing the halo-ed plaques.

There were several possibilities for how the combined predators were behaving in the mixed cultures – were they acting independently on the prey, in competition with each other at overlapping receptor sites, were the phage aiding in some way predation by the *Bdellovibrio,* or *vice versa,* was the phage acting as an opportunistic passenger, or were there subsets of the prey population that were susceptible to predation by each? The mathematical modelling allowed investigation of this beyond experimental limits. The model selection results revealed the presence of three subsets of the prey population, those

423 susceptible to both predators, and those resistant to predation by either the phage or the
424 *Bdellovibrio.*

425 The final model gave a good fit to the co-predation experimental data. Moreover,
426 when fitted to just the data sets containing the prey only and the single predators, the
427 resulting parameter values gave a very similar fit to the experimental data for the combined
428 predation conditions. As the final model does not contain any terms for direct interactions
429 between the two predators, combined with the fact that fitting to single predator data
430 predicts the combined predation results, we conclude that the two predators act
431 independently.

432 One question did remain to why did we isolate halo-ed plaques from the
433 environment which contained both predators, if they can operate independently? Clearly
434 during our dual predation experiments a final yield of c1 × 10^{10} phage were present from a
435 prey population which yielded c1 × 10^{6} *B. bacteriovorus*, so phage were in 10,000 fold
436 excess. High phage abundance was probably the reason for their presence in each plaque.
437 The rapid accumulation of phage resistant populations of *E. coli*, preyed upon by phage,
438 provides no barrier to *B. bacteriovorus* predation so does not prevent co-occurrence.

439 Purification of each predator made it possible to study their individual and combined
440 effects in ways not possible in other studies (43). Employing a low-nutrient environment
441 allowed predation by each predator, and allowed sustained viability of the *E. coli* population
442 over the 48 hours of investigation. Experimental predation by the *Bdellovibrio* alone
443 resulted in a gradual decrease in prey numbers from 1.2 × 10^{9} cfu/ml to a minimum of 2.0 ×
444 10^{4} cfu/ml (Fig. 2). This is consistent with other reports of *Bdellovibrio* predation on a variety
445 of different prey species where complete killing of the prey population was not observed
446 (26, 31, 33). The modelling revealed that a subpopulation of prey arose that would exhibit a

447 "plastic" resistance to *Bdellovibrio* predation, a form of resistance that is not genetically
448 encoded, and is also not passed to daughter cells, consistent with the "plastic" resistance
449 phenotype previously reported (24). It had previously been hypothesised (24) that this
450 resistance would arise due to the release of a molecular signal from the lysis of the
451 bdelloplast, and the modelling supports such a mechanism. This "plastic" resistance may
452 pose a problem if considering the therapeutic application of *Bdellovibrio* (3), as it may limit
453 the reduction of pathogen numbers, although the immune system has been shown to act
454 synergistically *in vivo* (12). In addition, physiological state of prey (leading to plastic
455 resistance or not) may be different in the *in vivo* growth conditions. Our modelling predicts
456 that, in a dual predation setting, the balance between applied predator numbers is
457 important and that adding sufficient but not excess phage with *B. bacteriovorus* gives the
458 best outcome.

459 Predation by the phage alone resulted in a 10-fold larger (but transient) decrease of
460 the prey population to 2.1×10^3 cfu/ml (seen at 6 hours, Fig. 2B), before phage-resistant
461 prey growth resulted in a final prey population at 48 hours similar to the starting
462 population. The model assumed the presence of a small fraction of phage resistant prey at
463 the beginning of the experiment; the median value of this fraction was 2.6×10^{-6} after fitting
464 (Table S1). This is similar in order of magnitude to previously reported values for *E. coli* (5,
465 40). The model evaluations indicated that the rise in bacteriophage-resistant prey resulted
466 both from growth of this initial, resistant population and spontaneous mutations arising in
467 members of the initially phage-sensitive prey population. Both were selected for during the
468 time course of the experiment. Replication of the phage-resistant prey resulted in the
469 production of phage-resistant progeny, consistent with resistance being the result of genetic
470 mutation. Sequencing of the phage resistant genomes points to the absence of the ferric

hydroxamate uptake, FhuA, protein as the reason for *E. coli* resistance to phage halo. This mutation would have little fitness effect in the iron-containing environment of our experimentation and given additional routes of iron uptake by *E. coli*.

The most noteworthy result of our study was the eradication of *E. coli* prey (reduction below detectable levels of less than 10 cells/ml) when preyed upon by both the *B. bacteriovorus* and the phage together (Fig. 2). The modelling revealed that the two predators were not interacting directly with each other as the experimental results could be recapitulated by the model using the data from the individual predators, without the need for the inclusion of any terms for direct interactions between predators. This suggests the potential for this phenomenon to be replicated for other combinations of Gram-negative prey, *B. bacteriovorus* and prey-specific bacteriophage, something that should be further investigated (beyond the scope of this paper). Such combinatorial predator therapy could be considered as a future alternative antibacterial treatment reducing bacterial numbers to lower levels than achievable with single predators alone, and reducing the selection for single predator-specific resistance.

MATERIALS AND METHODS

Bacterial strains, maintenance and isolation. *E. coli* S17-1 (44) prey were grown for 16 hours in YT broth (45) at 37°C with shaking at 200 rpm to late-log phase for use in predatory *Bdellovibrio* cultures (see below for predation kinetics description). *B. bacteriovorus* predatory cultures were set up as previously described and consisted of a mixture of Calcium HEPES buffer, *E. coli* culture and a previous *B. bacteriovorus* culture in a 50:3:1 v:v:v ratio (45) at 29°C with shaking at 200 rpm. Where stated, the *B. bacteriovorus* type strain HD100 (37, 46) was used for comparison. Host-independent (HI) *B. bacteriovorus* were grown as described in (45, 47), the HD100 derivative HID13 was described in (21) and the angelus HI strain was obtained as part of this study.

Bdellovibrio bacteriovorus strain angelus and bacteriophage halo were co-isolated using *E. coli* S17-1 as prey on YPSC double-layer agar plates as described previously (45). The bacteriophage halo was purified from the mixed phage-*B. bacteriovorus* cultures by growing the phage on *E. coli* S17-1 containing the plasmid pZMR100 (48) to confer resistance to kanamycin, which was added at 50 µg/ml, killing the Kn^S *B. bacteriovorus* angelus, using repeated rounds of plaque purification on YPSC overlay plates (45, 49). Phage resistant *E. coli* S17-1 were obtained by plating *E. coli* cells remaining in pure bacteriophage halo infection cultures and screening resultant isolates by addition of bacteriophage halo. These phage resistant *E. coli* (two strains F & G) were used to purify the *B. bacteriovorus* angelus from the originally mixed phage and *B. bacteriovorus* co-cultures, again using rounds of plaque purification. The resulting purified *B. bacteriovorus* angelus produced small plaques (smaller than those produced by the type strain HD100 under matched conditions) on both the phage resistant and original phage-sensitive *E. coli*.

510 ***Bdellovibrio*** **DNA purification and 16S rRNA sequencing.** To phylogenetically characterise
511 the pure *Bdellovibrio* strain isolated in the co-culture, *Bdellovibrio* genomic DNA was
512 purified from 0.45µm filtered host-dependently grown (before and after separation from
513 the associated phage) and unfiltered host-independently grown *B. bacteriovorus* angelus
514 using the Genelute Bacterial Genomic DNA Kit (Sigma) following the manufacturer's
515 instructions. The full-length 16S rRNA gene was amplified from a total of 11 individual
516 genomic DNA samples using Phusion high-fidelity polymerase (Finnzymes) following the
517 manufacturer's guidelines using general bacterial primers 8F (50) and 1492r (51). Purified
518 PCR products were sent for sequencing at MWG Biotech Ltd, and the full length double-
519 stranded sequence was aligned to that of the *Bdellovibrio bacteriovorus* type strain HD100
520 (37).
521
522 **Phage preparation and protein identification.** Phage preparations were made by addition
523 of bacteriophage halo (purified as described above and in the results) to a mid-log phase
524 culture of *E. coli* S17-1 (pZMR100) and incubated at 29^{o}C. When the optical density (OD) of
525 the culture at 600 nm dropped to half that of the starting OD, chloroform was added and
526 the phage particles were collected using PEG precipitation as described for lambda phage
527 (52).
528 Phage preparations were run on standard 12.5% acrylamide SDS polyacrylamide gels
529 (53) to examine their protein content; a single band was excised and analysed by MALDI
530 QToF MS, and the resulting peptide reads compared to existing sequences in NCBI
531 databases for the most significant hits.
532

533 **Phage and prey genomic DNA purification and sequencing.** Bacteriophage halo genomic
534 DNA was extracted from the above phage preparations using the Qiagen Lambda Maxi Kit
535 (Qiagen) following the manufacturer's instructions from step 6 to step 15. Harvested DNA
536 was resuspended in a final volume of 1 ml 10 mM Tris, 1 mM EDTA pH 7.5. Restriction-
537 digested fragments of phage genomic DNA were cloned into pUC19 (54) and sent for
538 sequencing at MWG Biotech Ltd using standard pUC19 primers M13uni(-21) and M13rev(-
539 29). To complete the phage sequence contig, unsequenced regions of cloned fragments
540 were PCR amplified using KOD high-fidelity polymerase, and purified PCR products sent for
541 sequencing. A 7 kb contig of phage genomic DNA was fully sequenced, compared to other
542 phage genomes by DNA and protein BLASTs at NCBI, and deposited in GenBank under
543 accession number GQ495225.

544 *E. coli* S17-1 genomic DNA was prepared using a Sigma GenElute Bacterial Genomic
545 DNA kit (Sigma- Aldrich Co, St Louis), from 16 hour overnight cultures of wild type and
546 phage resistant strains F and G. MinION and Illumina HiSeq platforms were used to
547 sequence the genome of *E. coli* S17-1 (4,772,290 nucleotides). Long-read sequences from
548 the MinION were used as a scaffold for Illumina data consisting of 4.6 million paired-end
549 sequence reads with lengths of 250 bp. Sequence assembly was performed using CLC
550 Genomics Workbench version 11.0.1 (Qiagen, Aarhus, Denmark). The genome sequence is
551 available under GenBank accession number CP040667. Phage resistant genome sequences
552 were assembled using the *E. coli* S17-1 chromosome as template from Illumina HiSeq data
553 composed of 0.8 and 3.5 million paired-end sequence reads of 250 bp for mutants F and G
554 respectively. These data also included the DNA sequence of plasmid pZMR100 (5,580
555 nucleotides).
556

557 **Electron microscopy.** *B. bacteriovorus* cells and phage preparations were visualised using
558 transmission electron microscopy. 15 µl of sample was placed on a carbon formvar grid
559 (Agar Scientific) for five minutes before being removed and 15 µl of 0.5% Uranyl Acetate
560 added for 1 minute before the grid was dried. Samples were imaged using a JEOL JEM1010
561 electron microscope.
562
563 **Predation kinetics experiments.** Predation kinetics were assayed as described and reasoned
564 in the results: experimental measurements were taken in triplicate and viable counting was
565 used to enumerate phage, *B. bacteriovorus* and *E. coli*. Two separate biological repeats of
566 the experiment were run over 48 hours, with enumerations of all three populations every
567 two hours by a team of four people.
568 The starting prey cultures had to be established by experimentation to produce prey
569 cells that were suitable for both *B. bacteriovorus* and phage predation. In the lab, *B.*
570 *bacteriovorus* predation is usually studied using stationary-phase prey, whilst phage
571 predation typically requires exponentially-growing prey; here our setup resulted in late-log
572 phase prey cells that were preyed upon by both predators. *E. coli* S17-1 prey cells were pre-
573 grown for 16 hours shaken at 37^{o}C in YT broth. They were added, still in the YT broth, to 100
574 ml of calcium HEPES buffer (2 mM $CaCl_2$ 25 mM HEPES pH 7.8) to give a final OD_{600nm} of 0.75
575 units (typically 20ml of overnight culture added to 100 ml buffer), resulting in an average
576 starting *E. coli* prey population in the experimental cultures of 2.9×10^8 cfu/ml.
577 Into 100 ml of this prey suspension, 2 ml of an attack-phase culture of *B.*
578 *bacteriovorus* HD100 was added (or 2 ml calcium HEPES buffer to *B. bacteriovorus* free
579 controls) giving an average starting *B. bacteriovorus* count in the experimental cultures of
580 2.8×10^6 pfu/ml. To this, 20 µl of a pure preparation of the halo-phage was added, giving an

581 average starting count in the experimental cultures of 3.7×10^6 pfu/ml. Cultures were
582 incubated at 29°C with shaking at 200 rpm, and samples taken every 2 hours.

583 At each timepoint, OD_{600nm} was measured and samples plated onto the appropriate
584 agar plates for enumeration of *E. coli* (YT), bacteriophage halo (YPSC with kanamycin at 50
585 µg/ml, with S17-1 pZMR100 prey) and *B. bacteriovorus* HD100 (YPSC with phage-resistant
586 S17-1 as prey).

587

588 **Mathematical modelling.** A family of ordinary differential equation (ODE) models were
589 developed to describe the population dynamics. ODEs were ideal as the experimental data
590 are at the population rather than the individual level and the ODE model can be solved
591 rapidly (this is important as we had to simulate the model millions of times for the model
592 selection and parameter inference). Fig. 3 visualizes the variables, their interactions and the
593 equations of the base model with one prey type. Fig. 4 does the same for the final model as
594 well as explaining the different model variants. Parameters are defined in Table S1. The full
595 sets of equations and details on the ODE solver are given in Supplemental Text. Each model
596 variant was fitted to the experimental data shown in Fig. 2. A Bayesian framework for model
597 selection and parameter inference was used to obtain estimates of the uncertainty of the
598 model and parameters. As explicit likelihood functions cannot be derived, an Approximate
599 Bayesian Computation (ABC) with Sequential Monte Carlo (ABC-SMC) algorithm was used as
600 described by Stumpf and co-workers (55), for details of the procedure see Supplemental
601 Text. Figs. S3 and S4 show how the fit improves with decreasing tolerance and Fig. S5 shows
602 how the accepted parameter ranges narrow down increasingly from the broad priors. The
603 objective choice of typical parameter sets via PCA is shown in Fig. S7. The open source code

for running the simulations and the model selection and fitting are available as Supplemental Code.

Accession numbers. The nucleotide sequences derived in this work have been deposited with GenBank. The bacteriophage halo partial genome sequence has accession number GQ495225.1 https://www.ncbi.nlm.nih.gov/nuccore/GQ495225 and the *B. bacteriovorus* angelus full-length 16S rRNA sequence has accession number GQ427200.1 https://www.ncbi.nlm.nih.gov/nuccore/GQ427200.1/.

The *E. coli* wild type strain S17-1 genome sequence was deposited with the accession number CP040667.1 https://www.ncbi.nlm.nih.gov/nuccore/NZ_CP040667.1

ACKNOWLEDGEMENTS

This work was carried out with contributions by many workers on the multi-day live experimentation and modelling sides. We thank Kevin Bailey for MALDI QToF MS analysis and peptide identification, Angus Davison and Richard Woods for helpful advice, Iain G. Johnston for guidance using ABC and Marilyn Whitworth for technical support. L.H., C.L., M.J.C., R.J.A. and R.T. were supported by HFSP grant RGP57/2005 and Biotechnology and Biological Sciences Research Council (BBSRC) UK grant BB/G003092/1. D.S.M., A.S., M.J.C., S.G. and A.L. were undergraduate students at University of Nottingham. D.S.M. was supported by a Nuffield Foundation undergraduate summer bursary and A.L. by an SGM undergraduate summer bursary. J.K.S. was supported by a BBSRC funded, Midlands Integrative Biosciences Training Partnership (MIBTP) PhD studentship. M.B., J.T., J.Tw. were supported by US Army Research Office and the Defense Advanced Research Projects Agency under Cooperative Agreement Number W911NF-15-2-0028 to R.E.S. The views and

conclusions contained in this document are those of the authors and should not be interpreted as representing the official policies, either expressed or implied, of the Army Research Office, DARPA, or the U.S. Government.

AUTHOR CONTRIBUTIONS

R.E.S devised the experimental work with L.H. and R.T.. Live experimental data collection was carried out by a group of experimental researchers: L.H., R.T., D.S.M., R.J.A., A.S., M.J.C., S.G. and A.L. J.K.S. and J.U.K. devised and J.K.S. carried out the modelling work with inputs from M.B., J.T. and J.Tw. C.L. and J.T. did nucleic acid sequencing and I.C. annotated and deposited the *E. coli* genome sequence. R.E.S., J.K.S., L.H., J.T. and J.U.K. drafted the manuscript with comments from M.B. All authors gave final approval for publication.

REFERENCES

1. Allen HK, Trachsel J, Looft T, Casey TA. 2014. Finding alternatives to antibiotics. Ann N Y Acad Sci 1323:91-100.
2. Lederberg J. 1996. Smaller fleas ... ad infinitum: therapeutic bacteriophage redux. Proc Natl Acad Sci U S A 93:3167-8.
3. Negus D, Moore C, Baker M, Raghunathan D, Tyson J, Sockett RE. 2017. Predator Versus Pathogen: How Does Predatory Bdellovibrio bacteriovorus Interface with the Challenges of Killing Gram-Negative Pathogens in a Host Setting? Annu Rev Microbiol 71:441-457.
4. Kakasis A, Panitsa G. 2018. Bacteriophage therapy as an alternative treatment for human infections. A comprehensive review. Int J Antimicrob Agents doi:10.1016/j.ijantimicag.2018.09.004.
5. Oechslin F. 2018. Resistance Development to Bacteriophages Occurring during Bacteriophage Therapy. Viruses 10.
6. Cairns BJ, Timms AR, Jansen VA, Connerton IF, Payne RJ. 2009. Quantitative models of in vitro bacteriophage-host dynamics and their application to phage therapy. PLoS Pathog 5:e1000253.
7. Weitz J. 2016. Quantitative Viral Ecology: Dynamics of Viruses and Their Microbial Hosts. Princeton University Press.
8. Gu J, Liu X, Li Y, Han W, Lei L, Yang Y, Zhao H, Gao Y, Song J, Lu R, Sun C, Feng X. 2012. A method for generation phage cocktail with great therapeutic potential. PLoS One 7:e31698.

9. Schooley RT, Biswas B, Gill JJ, Hernandez-Morales A, Lancaster J, Lessor L, Barr JJ, Reed SL, Rohwer F, Benler S, Segall AM, Taplitz R, Smith DM, Kerr K, Kumaraswamy M, Nizet V, Lin L, McCauley MD, Strathdee SA, Benson CA, Pope RK, Leroux BM, Picel AC, Mateczun AJ, Cilwa KE, Regeimbal JM, Estrella LA, Wolfe DM, Henry MS, Quinones J, Salka S, Bishop-Lilly KA, Young R, Hamilton T. 2017. Development and Use of Personalized Bacteriophage-Based Therapeutic Cocktails To Treat a Patient with a Disseminated Resistant Acinetobacter baumannii Infection. Antimicrob Agents Chemother 61.
10. Atterbury RJ, Hobley L, Till R, Lambert C, Capeness MJ, Lerner TR, Fenton AK, Barrow P, Sockett RE. 2011. Effects of orally administered Bdellovibrio bacteriovorus on the well-being and Salmonella colonization of young chicks. Appl Environ Microbiol 77:5794-803.
11. Shatzkes K, Singleton E, Tang C, Zuena M, Shukla S, Gupta S, Dharani S, Onyile O, Rinaggio J, Connell ND, Kadouri DE. 2016. Predatory Bacteria Attenuate Klebsiella pneumoniae Burden in Rat Lungs. MBio 7.
12. Willis AR, Moore C, Mazon-Moya M, Krokowski S, Lambert C, Till R, Mostowy S, Sockett RE. 2016. Injections of Predatory Bacteria Work Alongside Host Immune Cells to Treat Shigella Infection in Zebrafish Larvae. Curr Biol 26:3343-3351.
13. Ackermann HW. 2006. Classification of bacteriophages., p 8-16. *In* Calendar R (ed), The Bacteriophages. Oxford University Press, New York.
14. Shea TB, Seaman E. 1984. SP3: a flagellotropic bacteriophage of Bacillus subtilis. J Gen Virol 65 (Pt 11):2073-6.
15. Susskind MM, Botstein D. 1978. Molecular genetics of bacteriophage P22. Microbiol Rev 42:385-413.
16. Randall-Hazelbauer L, Schwartz M. 1973. Isolation of the bacteriophage lambda receptor from Escherichia coli. J Bacteriol 116:1436-46.
17. Koskella B, Meaden S. 2013. Understanding bacteriophage specificity in natural microbial communities. Viruses 5:806-23.
18. Coffey A, Ross RP. 2002. Bacteriophage-resistance systems in dairy starter strains: molecular analysis to application. Antonie Van Leeuwenhoek 82:303-21.
19. Stern A, Sorek R. 2011. The phage-host arms race: shaping the evolution of microbes. Bioessays 33:43-51.
20. Sockett RE. 2009. Predatory lifestyle of Bdellovibrio bacteriovorus. Annu Rev Microbiol 63:523-39.
21. Lambert C, Chang CY, Capeness MJ, Sockett RE. 2010. The first bite--profiling the predatosome in the bacterial pathogen Bdellovibrio. PLoS One 5:e8599.
22. Fenton AK, Kanna M, Woods RD, Aizawa SI, Sockett RE. 2010. Shadowing the actions of a predator: backlit fluorescent microscopy reveals synchronous nonbinary septation of predatory Bdellovibrio inside prey and exit through discrete bdelloplast pores. J Bacteriol 192:6329-35.
23. Koval SF, Hynes SH. 1991. Effect of paracrystalline protein surface layers on predation by Bdellovibrio bacteriovorus. J Bacteriol 173:2244-9.
24. Shemesh Y, Jurkevitch E. 2004. Plastic phenotypic resistance to predation by Bdellovibrio and like organisms in bacterial prey. Environ Microbiol 6:12-8.
25. Kadouri DE, To K, Shanks RM, Doi Y. 2013. Predatory bacteria: a potential ally against multidrug-resistant Gram-negative pathogens. PLoS One 8:e63397.

26. Sun Y, Ye J, Hou Y, Chen H, Cao J, Zhou T. 2017. Predation Efficacy of Bdellovibrio bacteriovorus on Multidrug-Resistant Clinical Pathogens and Their Corresponding Biofilms. Jpn J Infect Dis 70:485-489.
27. Cotter TW, Thomashow MF. 1992. Identification of a Bdellovibrio bacteriovorus genetic locus, hit, associated with the host-independent phenotype. J Bacteriol 174:6018-24.
28. Krysiak-Baltyn K, Martin GJ, Stickland AD, Scales PJ, Gras SL. 2016. Computational models of populations of bacteria and lytic phage. Crit Rev Microbiol 42:942-68.
29. Varon M, Zeigler BP. 1978. Bacterial predator-prey interaction at low prey density. Appl Environ Microbiol 36:11-7.
30. Crowley PH, Straley SC, Craig RJ, Culin JD, Fu YT, Hayden TL, Robinson TA, Straley JP. 1980. A Model of Prey Bacteria, Predator Bacteria, and Bacteriophage in Continuous Culture. Journal of Theoretical Biology 86:377-400.
31. Baker M, Negus D, Raghunathan D, Radford P, Moore C, Clark G, Diggle M, Tyson J, Twycross J, Sockett RE. 2017. Measuring and modelling the response of Klebsiella pneumoniae KPC prey to Bdellovibrio bacteriovorus predation, in human serum and defined buffer. Sci Rep 7:8329.
32. Dattner I, Miller E, Petrenko M, Kadouri DE, Jurkevitch E, Huppert A. 2017. Modelling and parameter inference of predator-prey dynamics in heterogeneous environments using the direct integral approach. J R Soc Interface 14.
33. Hobley L, King JR, Sockett RE. 2006. Bdellovibrio predation in the presence of decoys: Three-way bacterial interactions revealed by mathematical and experimental analyses. Appl Environ Microbiol 72:6757-65.
34. Wilkinson MH. 2001. Predation in the presence of decoys: an inhibitory factor on pathogen control by bacteriophages or bdellovibrios in dense and diverse ecosystems. J Theor Biol 208:27-36.
35. Summers JK, Kreft, J.U. 2019. Predation strategies of the bacterium Bdellovibrio bacteriovorus result in bottlenecks, overexploitation, minimal and optimal prey sizes. bioRxiv 621490.
36. Wietzorrek A, Schwarz H, Herrmann C, Braun V. 2006. The genome of the novel phage Rtp, with a rosette-like tail tip, is homologous to the genome of phage T1. J Bacteriol 188:1419-36.
37. Rendulic S, Jagtap P, Rosinus A, Eppinger M, Baar C, Lanz C, Keller H, Lambert C, Evans KJ, Goesmann A, Meyer F, Sockett RE, Schuster SC. 2004. A predator unmasked: life cycle of Bdellovibrio bacteriovorus from a genomic perspective. Science 303:689-92.
38. Feucht A, Heinzelmann G, Heller KJ. 1989. Irreversible binding of bacteriophage T5 to its FhuA receptor protein is associated with covalent cross-linking of 3 copies of tail protein pb4. FEBS Lett 255:435-40.
39. Hespell RB, Rosson RA, Thomashow MF, Rittenberg SC. 1973. Respiration of Bdellovibrio bacteriovorus strain 109J and its energy substrates for intraperiplasmic growth. J Bacteriol 113:1280-8.
40. Luria SE, Delbruck M. 1943. Mutations of Bacteria from Virus Sensitivity to Virus Resistance. Genetics 28:491-511.
41. Jeschke JM, Kopp M, Tollrian R. 2002. Predator functional responses: Discriminating between handling and digesting prey. Ecological Monographs 72:95-112.

42. Wilkinson MHF. 2006. Mathematical Modelling of Predatory Prokaryotes. *In* Jurkevitch E (ed), Predatory Prokaryotes. Springer, Berlin, Heidelberg.
43. Chen H, Laws EA, Martin JL, Berhane TK, Gulig PA, Williams HN. 2018. Relative Contributions of Halobacteriovorax and Bacteriophage to Bacterial Cell Death under Various Environmental Conditions. MBio 9.
44. Simon R, Priefer U, Puhler A. 1983. A Broad Host Range Mobilization System for Invivo Genetic-Engineering - Transposon Mutagenesis in Gram-Negative Bacteria. Bio-Technology 1:784-791.
45. Lambert C, Sockett RE. 2008. Laboratory maintenance of Bdellovibrio. Curr Protoc Microbiol Chapter 7:Unit 7B 2.
46. Stolp H, Starr MP. 1963. Bdellovibrio Bacteriovorus Gen. Et Sp. N., a Predatory, Ectoparasitic, and Bacteriolytic Microorganism. Antonie Van Leeuwenhoek 29:217-48.
47. Evans KJ, Lambert C, Sockett RE. 2007. Predation by Bdellovibrio bacteriovorus HD100 requires type IV pili. J Bacteriol 189:4850-9.
48. Rogers M, Ekaterinaki N, Nimmo E, Sherratt D. 1986. Analysis of Tn7 transposition. Mol Gen Genet 205:550-6.
49. Lambert C, Smith MC, Sockett RE. 2003. A novel assay to monitor predator-prey interactions for Bdellovibrio bacteriovorus 109 J reveals a role for methyl-accepting chemotaxis proteins in predation. Environ Microbiol 5:127-32.
50. Hicks RE, Amann RI, Stahl DA. 1992. Dual staining of natural bacterioplankton with 4',6-diamidino-2-phenylindole and fluorescent oligonucleotide probes targeting kingdom-level 16S rRNA sequences. Appl Environ Microbiol 58:2158-63.
51. Kane MD, Poulsen LK, Stahl DA. 1993. Monitoring the enrichment and isolation of sulfate-reducing bacteria by using oligonucleotide hybridization probes designed from environmentally derived 16S rRNA sequences. Appl Environ Microbiol 59:682-6.
52. Perbal B. 1988. A Practical Guide to Molecular Cloning, 2 ed. Wiley Interscience.
53. Laemmli UK. 1970. Cleavage of structural proteins during the assembly of the head of bacteriophage T4. Nature 227:680-5.
54. Yanisch-Perron C, Vieira J, Messing J. 1985. Improved M13 phage cloning vectors and host strains: nucleotide sequences of the M13mp18 and pUC19 vectors. Gene 33:103-19.
55. Toni T, Welch D, Strelkowa N, Ipsen A, Stumpf MP. 2009. Approximate Bayesian computation scheme for parameter inference and model selection in dynamical systems. J R Soc Interface 6:187-202.

Figure Legends

Fig. 1. Unique halo-ed plaque morphology from which the co-isolated novel *B. bacteriovorus* angelus and bacteriophage halo were identified by electron microscopy. (A) Halo-ed plaques containing both *B. bacteriovorus* angelus and bacteriophage halo on lawns of *E. coli* in YPSC double-layer agar plates. Scale bar = 1 cm. **(B)** Electron microscopy of *B. bacteriovorus* angelus, stained with 0.5% URA pH 4.0. Scale bar = 500 nm. **(C)** Electron microscopy of a 0.22 µm filtrate of a predatory culture, showing the presence of phage

particles with curved tails resembling bacteriophage RTP. Phage were stained with 0.5% URA pH 4.0. Scale bar = 50 nm

Fig. 2. Kinetics of predation. Measured over 48 hours on late log-phase *E. coli* S17-1 by bacteriophage halo alone (green), *B. bacteriovorus* HD100 alone (red); both bacteriophage halo and *B. bacteriovorus* HD100 combined (purple) versus *E. coli* plus buffer control (blue). **(A)** *E. coli* measured by optical density (OD_{600nm}) (*B. bacteriovorus* are too small to register at OD_{600nm}). **(B)** *E. coli* viable counts. **(C)** *B. bacteriovorus* HD100 enumeration by plaque counts. **(D)** bacteriophage halo enumeration by plaque counts.

Fig. 3. Base model with one prey type. (A) Diagram of the model variables (populations and chemicals) in circles and their positive or negative interactions. The arrow colours match the colours of the terms in the equations in panel (B) and the roman numerals refer to the list of processes in the main text. **(B)** The set of differential equations defining the base model.

Fig. 4. Final model and model variants. (A) Diagram of the final model variables (populations and chemicals) and their positive or negative interactions. The arrow colours match the colours of the terms in the equations in panel (B). **(B)** The set of differential equations defining the final model. **(C)** Top level model variants with different prey phenotypes (models N1, N2, N3, N4). **(D)** Mid level model variants – **(Di)** methods of development of plastic resistance to *B. bacteriovorus*, **(Dii)** methods of development of phage resistance. **(E)** Low level model variants – predation rate either saturates at high prey densities or not (can differ between *B. bacteriovorus* and phage).

Fig. 5. Hierarchical model selection process. This infers which model variants from Fig. 4 are best supported by the data (frequency of a variant winning out of 1000). **(A)** Competition of models with different number of prey phenotypes. N1: one prey type sensitive to both predators (N_S), N2: two prey types, N_S and phage resistant prey (N_R), N3: three prey types, N_S and N_R and prey with plastic phenotypic resistance to *B. bacteriovorus* (N_P). N4: four prey types, N_S, N_R, N_P and prey with dual resistance (N_D). **(B)** Competition of models with different ways of converting between sensitive prey (N_S) and plastic resistant prey (N_P) but the same saturating *B. bacteriovorus* attack rate (Pii) and non-saturating phage attack rate (Vi). N3-IG-Pii-Vi: N_S intrinsically (spontaneously) converts to N_P and back conversion is coupled to growth. N3-S-Pii-Vi: N_S conversion to N_P is triggered by a signal and back conversion is spontaneous. N3-I-Pii-Vi: spontaneous conversion both ways. **(C)** The combined variant from panel (B) is in the middle and its 'parent' variants on either side. N3-SG-Pii-Vi: N_S conversion to N_P is triggered by a signal and back conversion is coupled to growth. **(D)** Model variants, derived from the combined model in panel (C), but differing in the way the signal is produced. N3-SBG-Pii-Vi: Signal derives from interaction of prey and *B. bacteriovorus* only. N3-SG-Pii-Vi: Signal derives from interaction of prey with both predators. N3-SVG-Pii-Vi: Signal derives from prey interaction with virus (phage) only. **(E)** Different ways of generating phage resistance. Phage resistant prey were already present initially or prey developed resistance *de novo* or both. **(F)** Model variants, based on N3-SBG from panel (D), but differing in attack rate saturation. Pii: *B. bacteriovorus* attack rate saturates at high prey density while Pi does not saturate. Likewise with Vii and Vi for the virus (phage). **(G)** Mortality of *B. bacteriovorus* (phage assumed to be stable) was either set to Hespell et al.

(1974) or fitted by the ABC-SMC method. Less decisive competitions (B-D) were repeated 10 times, see Fig. S6.

Fig. 6. Comparison of experimental data (mean values) with fits of the best model variant (from Fig. 5). The model was either fitted using **(A-D)** all experimental data or **(E-H)** all data without dual predation and then used to predict the outcome of dual predation (shown in H). The parameter values for each case are given in Table S1. Experimental data is shown by symbols, lines represent model simulations. **(A-H)** Blue: *E. coli* prey, Red: *B. bacteriovorus*, Green: bacteriophage halo, Pink: medium (not experimentally measured). **(I-L)** Dynamics of the sub-populations of prey and predators predicted by the model that was fitted to all data, corresponding to panels (A-D). **(I-L)** Blue: *E. coli* prey: solid line – susceptible prey N_S, dotted line – plastic resistant prey N_P, dashed line – bacteriophage resistant prey N_R. Red: *B. bacteriovorus*: solid line – free *B. bacteriovorus* P, dashed line – bdelloplasts B. Green: bacteriophage halo: solid line – free bacteriophage V, dashed line – bacteriophage-infected cells I. Pink: medium.

Table Legends

Table 1. Mutational changes present in the genome sequences of the bacteriophage resistant mutants

Table 1
Mutational changes present in the genome sequences of the bacteriophage resistant mutants

Accession number	Gene product	Nucleotide position	Changes in coding region	Reading frame change	Mutant isolates
FGH86_13085	KdbD TCS sensor histidine kinase	2690204	G to A substitution	D571N	F & G
FGH86_16680	FhuA Ferric hydroxamate transporter/ Phage receptor	3364483	IS4-like insertion	inactivation	F
FGH86_16680	FhuA Ferric hydroxamate transporter/ Phage receptor	3365489	IS4-like insertion	inactivation	G
FGH86_19640	Paraslipin	4005457	C to T substitution	S25F	F & G
FGH86_19645	Ribosome release factor	4005510	A to G substitution	-	F & G

Mutations in mutants F and G are presented relative to the reference chromosome sequence of *E. coli* S17-1 (CP040667).

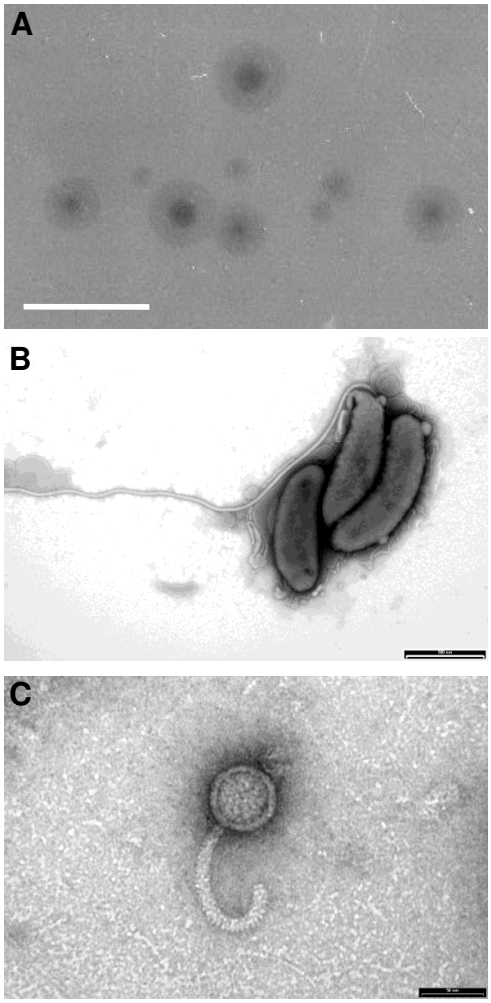

Fig. 1. Unique halo-ed plaque morphology from which the co-isolated novel *B. bacteriovorus* angelus and bacteriophage halo were identified by electron microscopy. (A) Halo-ed plaques containing both *B. bacteriovorus* angelus and bacteriophage halo on lawns of *E. coli* in YPSC double-layer agar plates. Scale bar = 1 cm. **(B)** Electron microscopy of *B. bacteriovorus* angelus, stained with 0.5% URA pH 4.0. Scale bar = 500 nm. **(C)** Electron microscopy of a 0.22 µm filtrate of a predatory culture, showing the presence of phage particles with curved tails resembling bacteriophage RTP. Phage were stained with 0.5% URA pH 4.0. Scale bar = 50 nm.

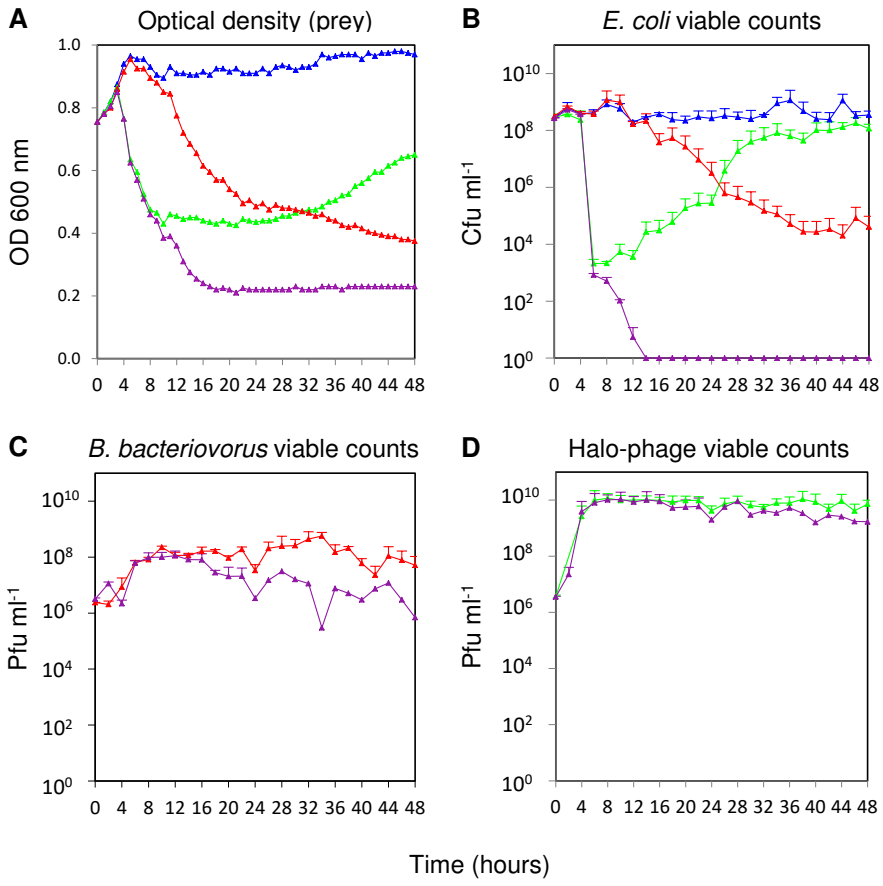

Fig. 2. Kinetics of predation. Measured over 48 hours on late log-phase *E. coli* S17-1 by bacteriophage halo alone (green), *B. bacteriovorus* HD100 alone (red); both bacteriophage halo and *B. bacteriovorus* HD100 combined (purple) versus *E. coli* plus buffer control (blue). **(A)** *E. coli* measured by optical density (OD_{600nm}) (*B. bacteriovorus* are too small to register at OD_{600nm}). **(B)** *E. coli* viable counts. **(C)** *B. bacteriovorus* HD100 enumeration by plaque counts. **(D)** bacteriophage halo enumeration by plaque counts.

A Base model variables and interactions

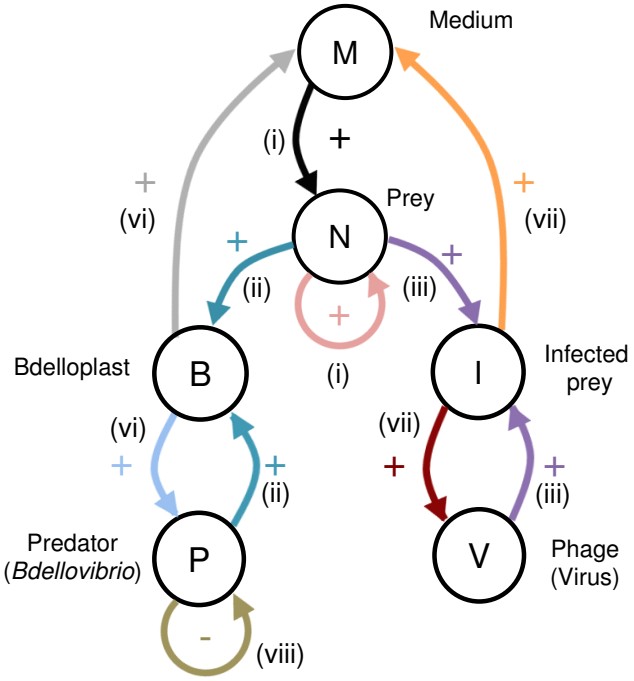

B Differential Equations (colours match arrows)

Rate of change	(i) Prey growth	(iv) Bdelloplast maturation	(ii) *Bdellovibrio* predation	(v) Infected prey *maturation*	(iii) Phage predation	(viii) *Bdello-vibrio* mortality	(vi) **and** (vii) Nutrient release
$\frac{dM}{dt} =$	$-N\frac{\mu_N M}{(K_{M,N}+M)Y_{N/M}}$						$+Y_{M/P}k_P B$ $+Y_{M/V}k_V I$
$\frac{dN}{dt} =$	$N\frac{\mu_N M}{K_{M,N}+M}$		$-P\frac{\mu_P N}{(K_{N,P}+N)Y_{B/N}}$		$-V\frac{\mu_V N}{Y_{I/V}}$		
$\frac{dP}{dt} =$		$k_P B$	$-P\frac{\mu_P N}{(K_{N,P}+N)Y_{B/P}}$			$-mP$	
$\frac{dB}{dt} =$		$-\frac{k_P B}{Y_{P/B}}$	$+P\frac{\mu_P N}{K_{N,P}+N}$				
$\frac{dV}{dt} =$				$k_V I - V\frac{\mu_V N}{Y_{I/V}}$			
$\frac{dI}{dt} =$				$-\frac{k_V I}{Y_{V/I}} + V\mu_V N$			

Fig. 3. Base model with one prey type. (A) Diagram of the model variables (populations and chemicals) in circles and their positive or negative interactions. The arrow colours match the colours of the terms in the equations in panel (B) and the roman numerals refer to the list of processes in the main text. (B) The set of differential equations defining the base model.

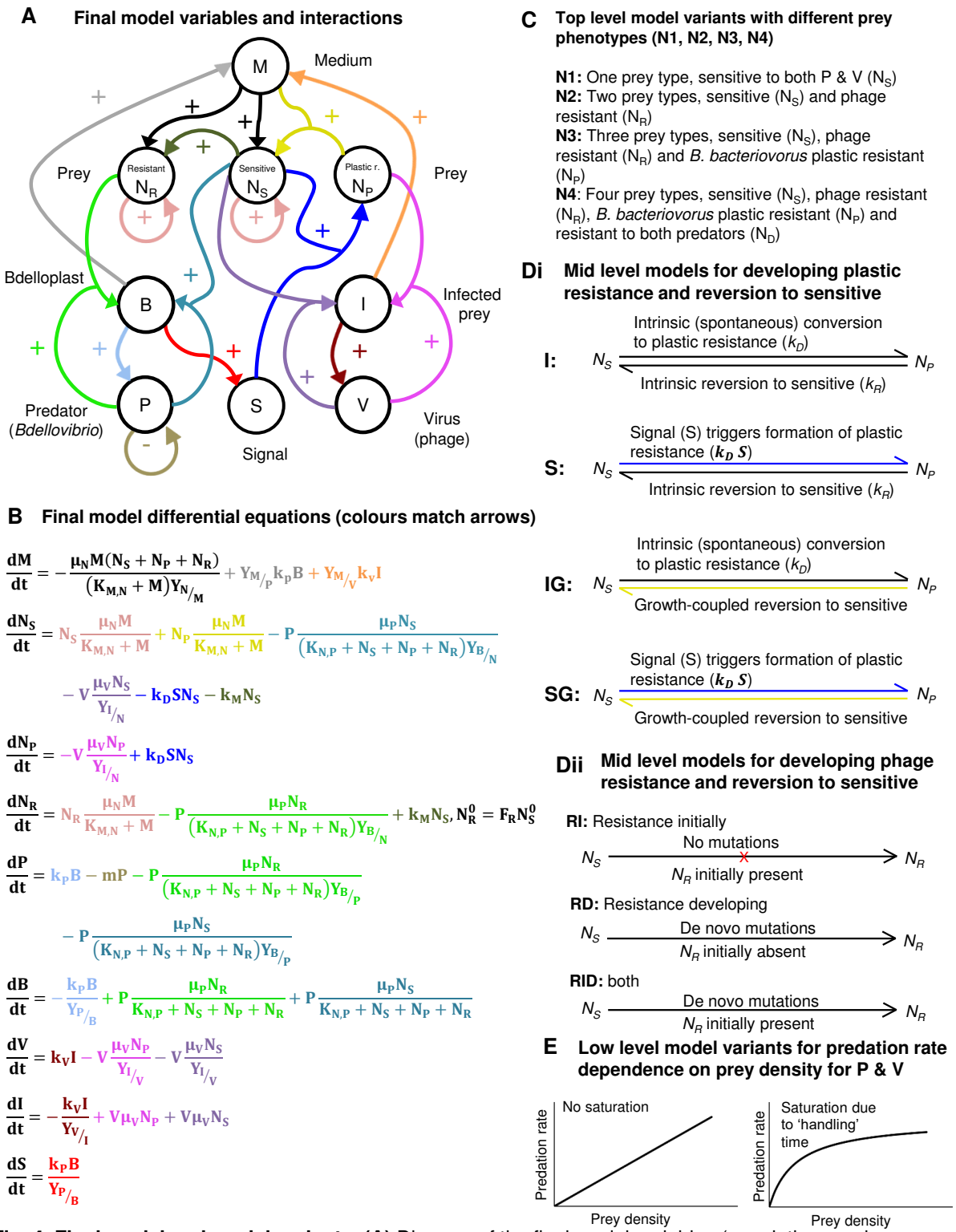

Fig. 4. Final model and model variants. (A) Diagram of the final model variables (populations and chemicals) and their positive or negative interactions. The arrow colours match the colours of the terms in the equations in panel (B). **(B)** The set of differential equations defining the final model. **(C)** Top level model variants with different prey phenotypes (models N1, N2, N3, N4). **(D)** Mid level model variants – **(Di)** methods of development of plastic resistance to *B. bacteriovorus*, **(Dii)** methods of development of phage resistance. **(E)** Low level model variants – predation rate either saturates at high prey densities or not (can differ between *B. bacteriovorus* and phage).

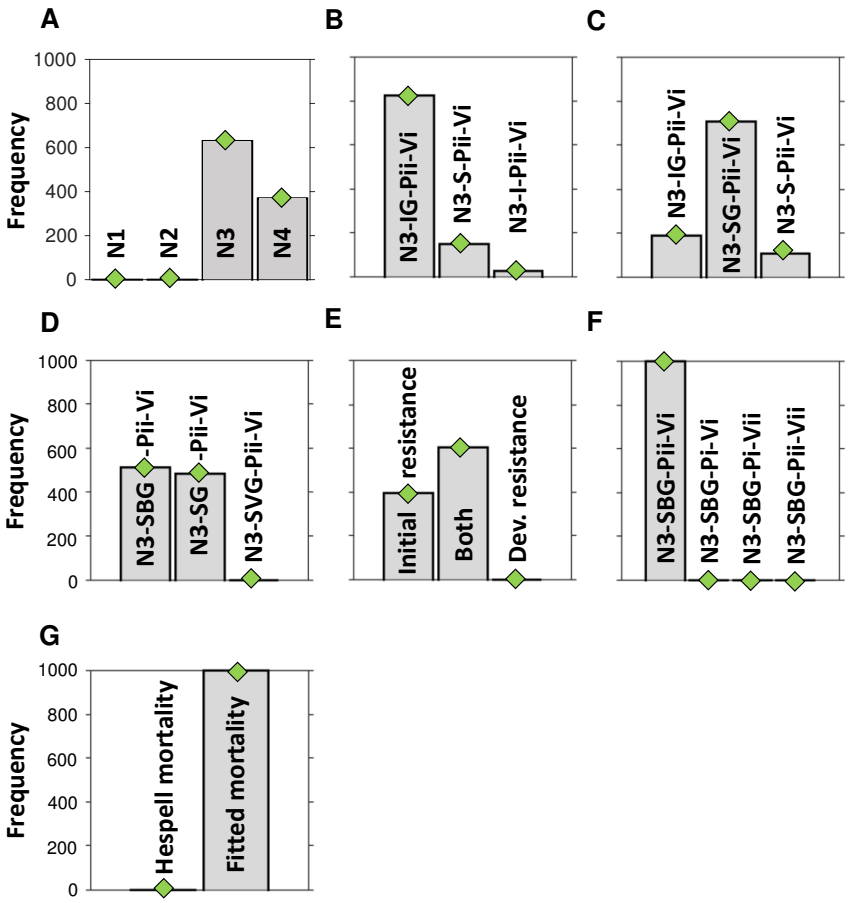

Fig. 5. Hierarchical model selection process. This infers which model variants from Fig. 4 are best supported by the data (frequency of a variant winning out of 1000). **(A)** Competition of models with different number of prey phenotypes. N1: one prey type sensitive to both predators (N_S), N2: two prey types, N_S and phage resistant prey (N_R), N3: three prey types, N_S and N_R and prey with plastic phenotypic resistance to *B. bacteriovorus* (N_P). N4: four prey types, N_S, N_R, N_P and prey with dual resistance (N_D). **(B)** Competition of models with different ways of converting between sensitive prey (N_S) and plastic resistant prey (N_P) but the same saturating *B. bacteriovorus* attack rate (Pii) and non-saturating phage attack rate (Vi). N3-IG-Pii-Vi: N_S intrinsically (spontaneously) converts to N_P and back conversion is coupled to growth. N3-S-Pii-Vi: N_S conversion to N_P is triggered by a signal and back conversion is spontaneous. N3-I-Pii-Vi: spontaneous conversion both ways. **(C)** The combined variant from panel (B) is in the middle and its 'parent' variants on either side. N3-SG-Pii-Vi: N_S conversion to N_P is triggered by a signal and back conversion is coupled to growth. **(D)** Model variants, derived from the combined model in panel (C), but differing in the way the signal is produced. N3-SBG-Pii-Vi: Signal derives from interaction of prey and *B. bacteriovorus* only. N3-SG-Pii-Vi: Signal derives from interaction of prey with both predators. N3-SVG-Pii-Vi: Signal derives from prey interaction with virus (phage) only. **(E)** Different ways of generating phage resistance. Phage resistant prey were already present initially or prey developed resistance *de novo* or both. **(F)** Model variants, based on N3-SBG from panel (D), but differing in attack rate saturation. Pii: *B. bacteriovorus* attack rate saturates at high prey density while Pi does not saturate. Likewise with Vii and Vi for the virus (phage). **(G)** Mortality of *B. bacteriovorus* (phage assumed to be stable) was either set to Hespell et al. (1974) or fitted by the ABC-SMC method. Less decisive competitions (B-D) were repeated 10 times, see Fig. S6.

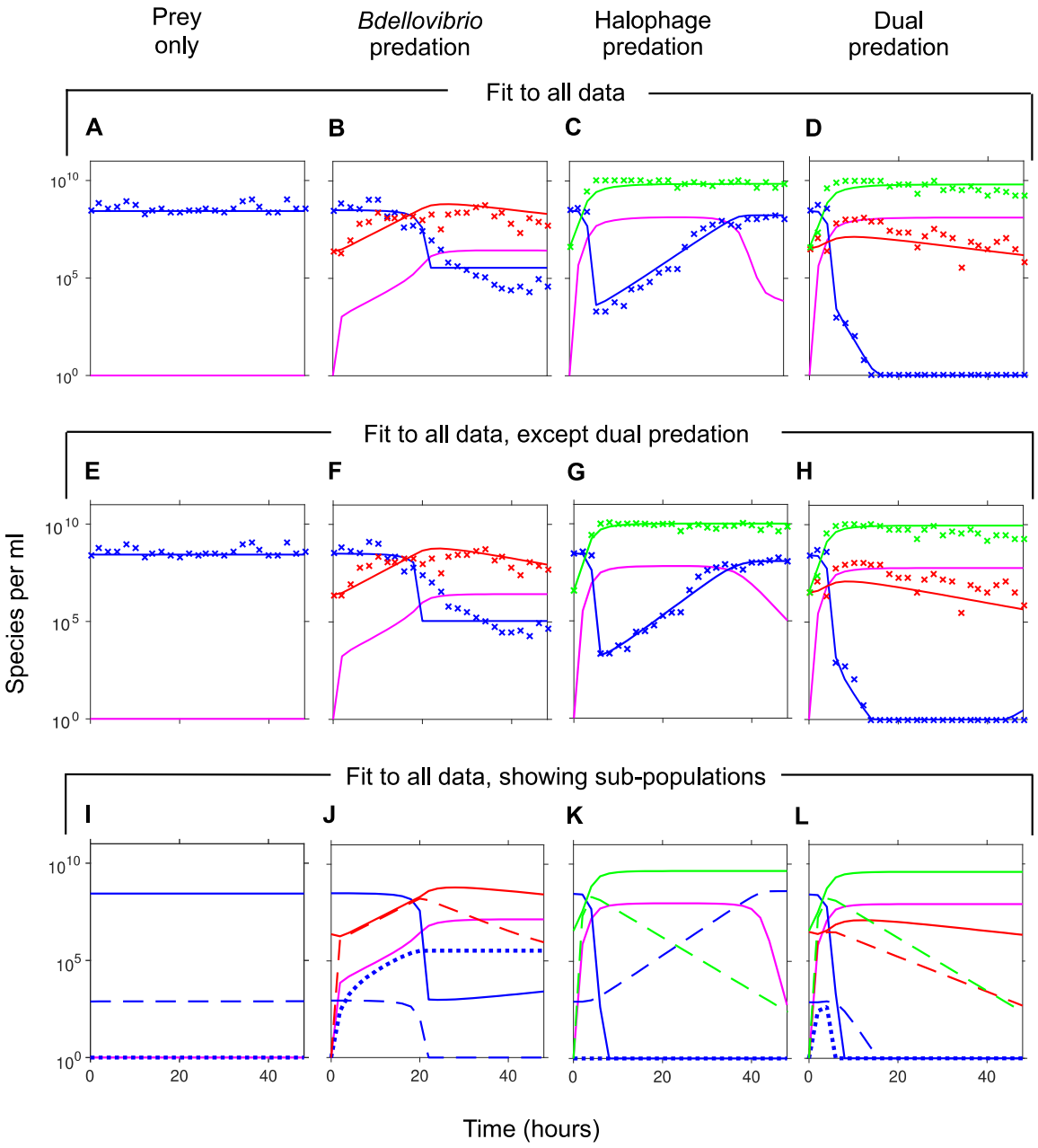

Fig. 6. Comparison of experimental data (mean values) with fits of the best model variant (from Fig. 5). The model was either fitted using **(A-D)** all experimental data or **(E-H)** all data without dual predation and then used to predict the outcome of dual predation (shown in H). The parameter values for each case are given in Table S1. Experimental data is shown by symbols, lines represent model simulations. **(A-H)** Blue: *E. coli* prey, Red: *B. bacteriovorus*, Green: bacteriophage halo, Pink: medium (not experimentally measured). **(I-L)** Dynamics of the sub-populations of prey and predators predicted by the model that was fitted to all data, corresponding to panels (A-D). **(I-L)** Blue: *E. coli* prey: solid line – susceptible prey N_S, dotted line – plastic resistant prey N_P, dashed line – bacteriophage resistant prey N_R. Red: *B. bacteriovorus*: solid line – free *B. bacteriovorus* P, dashed line – bdelloplasts B. Green: bacteriophage halo: solid line – free bacteriophage V, dashed line – bacteriophage-infected cells I. Pink: medium.